Available online at www.sciencedirect.com
SCIENCE DIRECT®
Solid State Communications 131 (2004) 319–323
solid state communications
www.elsevier.com/locate/ssc

Investigation of the variation in weak-link profile of $YBa_2Cu_{3-x}Ag_xO_{7-\delta}$ superconductors by Ag doping concentration

M. Tepe[a,*], I. Avci[a,b], H. Kocoglu[a], D. Abukay[b]

[a]*Department of Physics, Ege University, Faculty of Science, 35100 Bornova, Izmir, Turkey*
[b]*Department of Physics, Faculty of Science, Izmir Institute of Technology, 35436 Urla Campus, Izmir, Turkey*

Received 9 February 2004; received in revised form 22 March 2004; accepted 12 May 2004 by H. von Lohneysen
Available online 25 May 2004

Abstract

The effect of Ag doping concentration on the microstructure, transport properties and weak-link profile of $YBa_2Cu_{3-x}Ag_xO_{7-\delta}$ bulk superconducting compound was investigated through resistance–temperature ($R-T$), ac magnetic susceptibility ($\chi - T$), scanning electron microscope (SEM), X-ray diffraction (XRD) and the critical current density (J_c) versus applied magnetic field ($J_c - B$) measurements. We used the additive method with cationic ratio of $x = 0.1 - 0.4$ for the YBCO-Ag system. The change in the silver doping concentration slightly affected the transition temperatures ($T_{c,zero}$), whereas, the critical current densities (J_c) of the samples and their magnetic field (B) dependencies were noticeably affected. The improvement on the microstructural properties of YBCO bulk superconductors was observed in SEM analysis, the J_c values increased and their magnetic field dependencies decreased with the increasing of Ag concentration up to $x = 0.2$. As well as the current transport properties. Ag doping up to a certain amount produces texturing that gives rise to a modification in the weak-link profile resulting in an enhanced strength of flux pinning which causes an increase in the current carrying capacity.

PACS: 74.72.Bk; 74.62.Dh; 74.60.Jg; 74.25.Fy

Keywords: A. High-T_c Y-based superconductors; D. Ag doping; D. Weak-links; D. Transport properties

1. Introduction

The effect of doping on the superconducting YBCO ceramics has been extensively studied in order to improve their mechanical, structural and superconducting properties. The interest in doping has focused on Ag due to its good results obtained in improving the performance of YBCO [1–8]. The advantages of silver doping may be related to its ability in the enhancement of the critical current density and grain growth. Generally, it is believed that Ag diffuses into the grain boundary as a metal during thermal processing and it is responsible for the increasing interconnections between the grains [7]. This suggests that the amount of weak links in the structure is decreased by the improved interconnections and the pinning centers are improved achieving higher critical current density. It is also known that silver improves the grain orientation and oxygen diffusion during the final formation of the 1–2–3 phase [8]. Many studies have been made for the influence of Ag doping into the YBCO by different processes. An increase in the critical current density has been observed by Mendoza et al. [5]. The study related to the destruction in the grain boundaries and the enhancement in the critical current density by electrochemical Ag doping has been made by Matsumoto et al. [7]. The improvement in the grain structure of YBCO strongly depends upon the amount of Ag added. The excess concentration of Ag plays an important role as of preventive factor on the increasing of the grain sizes. Enough amount of Ag is responsible for the providing interconnection between the grains by filling into the pores in the structure. During the thermal processing, liquid silver fills into the pores because of the processing temperature of YBCO are

* Corresponding author. Tel.: +90-232-3884-000; fax: +90-232-388-10-36.
E-mail address: tepe@sci.ege.edu.tr (M. Tepe).

0038-1098/$ - see front matter © 2004 Published by Elsevier Ltd.
doi:10.1016/j.ssc.2004.05.015

significantly higher than the melting point of silver. It has been found that Ag neither affects the orthorhombic structure of YBCO nor reacts with or replaces any of its constituents [6].

The *c*-axis alignment of the structure is improved by the Ag addition up to a certain amount, thus improving the superconducting properties. With the excess amount of doping, the size of YBCO grains and their the *c*-axis orientations diminish, thus causes J_c to decrease. The investigation of the field dependence of the critical current density J_c is a very efficient tool in revealing the effect of weak-links and pinning centers in superconductors. The J_c as function of magnetic field (B) decreases with a certain amount of Ag doping but rapidly increases with the excess Ag concentration. In this study, we investigated the effect of Ag doping concentration with cationic ratios of $x = 0.1 - 0.4$ on the transport properties and weak-link profile of YBCO by optimizing the preparation process. The characterization of the samples carried out by ac susceptibility, $R-T$, $J_c - B_a$, SEM and XRD measurements.

2. Experimental

The pure and Ag-doped $YBa_2Cu_3O_{7-\delta}$ samples were prepared by the conventional solid-state reaction method under identical conditions. Y_2O_3(99.99%), BaO(99.99%), CuO(99.99%) and Ag_2O(99.99%) powders were used as the starting materials. The powders with the molar ratio of Y:Ba:Cu:Ag = 1:2:3 − x:x ($x = 0.00 - 0.40$) were mechanically well mixed for 1 h in an agate mortar and then were calcined twice at 920 °C for 24 h. The calcined materials were reground finely and pressed into pellets of 10 mm diameter at 400 MPa. The pellets were sintered in air at 950 °C for 50 h in a tabular furnace and then cooled down to room temperature a rate of 2 °C/min. The heat treatment processes of all samples were performed in alumina crucibles. The sample names were denoted as sample A, B, C, D and E depending on the doping concentrations of $x = 0.0$, 0.1, 0.2, 0.3 and 0.4, respectively.

The ac electrical resistance measurements were made by using standard four-probe method and measured by a two phase SR 530 Lock-in amplifier in the liquid nitrogen cryostat. The temperature of the samples was monitored by a calibrated Lakeshore Pt-thermometer. For J_c versus B measurements, the bulk samples were cut into rectangular bars from the pellets and they were thinned by using abrasive papers. The $J_c - B$ measurements were made using a standard four-probe method, and contacts were made by using silver paste. For magnetic fields between 7.6 and 45.6 mT, a copper wire solenoid was used and field direction was kept perpendicular to the measuring current direction. For the critical current a 1 μV/cm criterion was employed. X-ray diffraction patterns of the samples were obtained in the range of $2\theta = 3$ to 60°. SEM micrographs for the study of surface morphology of the samples were obtained using a XL 30S FEG SEM. The ac magnetic susceptibilities ($\chi' - i\chi''$) of the samples were measured by mutual inductance bridge, using a two phase SR 530 Lock-in amplifier to pick up in-phase (χ') and out-of-phase (χ'') signals of secondary coils.

3. Results and discussion

Fig. 1 shows the resistive transition ($R-T$) of the samples. It is clearly seen from the curves that the transition temperatures were slightly changed by the Ag content. As indicated in the inset in Fig. 1, the transition temperatures of the samples varied from 87 to 90 K with the increase in Ag concentration (up to $x = 0.2$, sample B and C). For the samples D and E ($x = 0.3$ and 0.4), $T_{c,zero}$ decreased down to below 87 K. The normal state resistances of the samples decrease linearly as the concentration of silver increases up to $x = 0.2$. As Ag fills the space between the YBCO grains, hence decreasing the porosity of the superconducting sample, this leads to a short-circuiting of the grains in the normal state.

The ac magnetic susceptibilities of the samples were measured in ac field of 10 A/m with a frequency of 1 kHz in the temperature range of 77–125 K. The inductive (χ', or in-phase) and resistive (χ'', or out-of-phase) components are shown in Fig. 2, which indicates that the diamagnetic transition temperatures are slightly different in values with varying Ag concentration. The pure sample showed the superconducting transition at $T_c = 89$ K. Although the diamagnetic transition temperature shifted to 92 K for the sample B ($x = 0.1$), the strongest diamagnetic behavior was observed for the sample C ($x = 0.2$) at T_c of 90 K. The diamagnetic saturation occurs at the temperature below of 85 K for the sample B, indicating the effect of weak-link in this sample. As seen from the Fig. 2, the curve of this sample exhibits a tail between the temperature range of

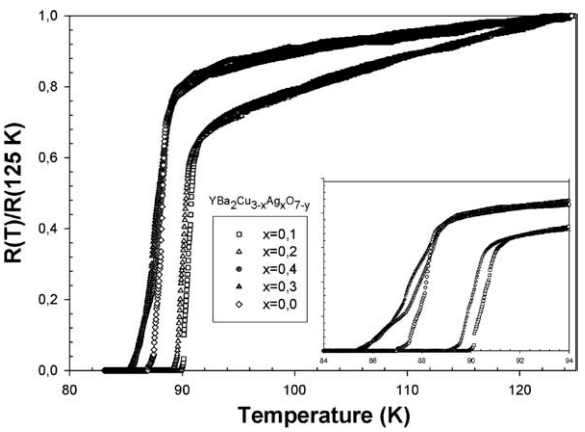

Fig. 1. Reduced resistance–temperature curves of pure and Ag doped YBCO samples.

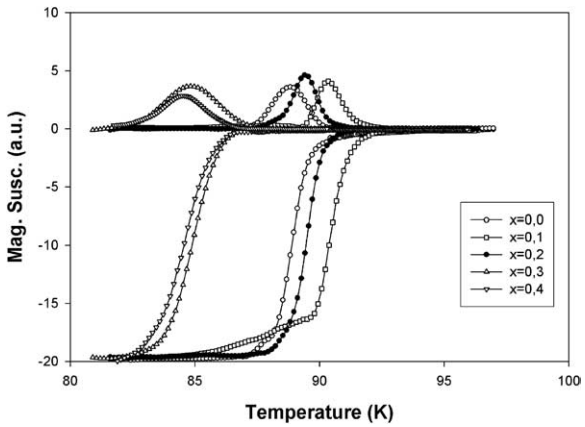

Fig. 2. AC magnetic susceptibility–temperature curves of pure and Ag doped YBCO samples.

85–90 K. However, the sample C has very sharp diamagnetic transition at 90 K, thus showing a very homogeneous YBCO phase. Decrease of the diamagnetic transition temperatures was also observed for the samples D and E. For these samples, the diamagnetic transition temperatures shifted to lower values than that of the pure sample. This means that the doping concentration above $x = 0.2$ causes a degradation on the superconducting properties of grain boundaries and their alignments, thus lowering the diamagnetic response of the YBCO compound. The results of the resistance and susceptibility measurements indicate that the optimized amount of Ag doping improves the transition temperature and diamagnetic behavior of YBCO composites but exceeding that value results in degradation on these properties.

Fig. 3 shows the XRD patterns of pure and YBCO-Ag samples. As we expect, the XRD patterns for the sample C showed an improvement in *c*-axis orientation. But also we observed that the phases appeared in samples with low Ag begin to disappear as doping level goes up to $x = 0.2$ and increasing again with the Ag content above $x = 0.2$. The lattice parameters for all samples did not deviate from an orthorhombic cell, thus indicating Ag neither affects the orthorhombic structure of the YBCO nor reacts with or replaces any of its constituents.

Fig. 4 shows the surface morphologies of the pure and YBCO-Ag composites obtained by scanning electron microscopy (SEM). In Fig. 4(a), the morphology of the pure sample is shown. The grain structure and the porosity of this sample are typical for the YBCO pelletized at the pressure of 400 MPa. It is clearly seen from the micrographs that the grain sizes and their orientation were improved with the Ag addition up to a certain amount. As Ag concentration increases up to $x = 0.2$, (in Fig. 4(b) and (c)), the grains become larger and oriented more orderly and the structure becomes almost non-porous. It can be noticed that the sample C has the highest bulk density and the grains in that sample are strongly linked. As Ag concentration exceeds

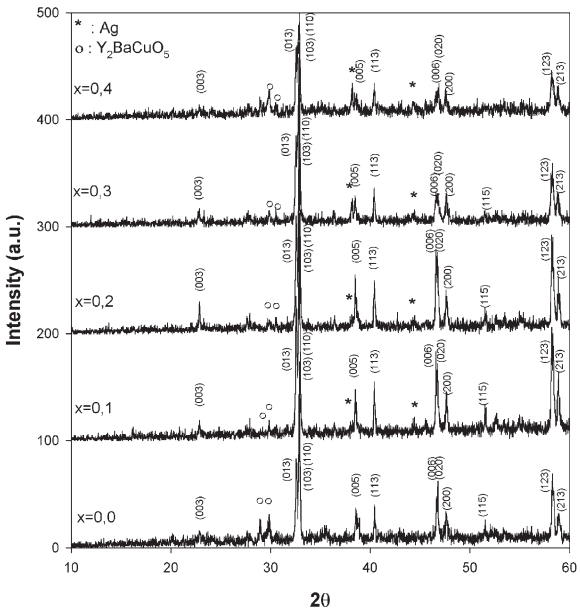

Fig. 3. XRD patterns of pure and Ag doped YBCO samples.

optimum value, $x = 0.2$, (in Fig. 4(d) and (e)), the structure becomes more porous than the pure sample and the grain sizes significantly decrease. Here we believe the excess Ag addition (above the concentration of $x = 0.2$) prevents the growth of YBCO grains, thus resulting in degradation on superconducting properties of the samples.

Fig. 5 a shows the magnetic field (B) dependence of the critical current density (J_c) for all samples. It is found that, a strong increase of J_c was obtained for the sample C with an enhancement factor of 169% at 77 K and $B = 0$ mT. There exists a strong correlation between the Ag content and the J_c enhancement, thus showing that the Ag content, up to a certain amount, is responsible for improving the superconducting properties of YBCO composites. This enhancement in J_c depends on strongly linking of the YBCO grains by Ag resulting in a modification of defect nature in the grain boundaries besides filling the pores in the structure. The increase of grain sizes and their orientations in the samples as the increasing of doping level (seen in SEM micrographs) are also thought to be responsible for the J_c enhancement. However, the Ag concentration above $x = 0.2$, the size of YBCO grains decreases and their orientations become more arbitrary. All these effects cause a decrease in J_c significantly. As seen from the Fig. 5(b), the critical current densities increased with Ag content up to $x = 0.2$ and rapidly decreased above this value. This shows us that the Ag doping improves the grain boundary structure up to a certain degree, thus improving the superconducting properties; hence give higher critical current densities. In contrary, in the case of excess doping concentration, Ag impedes the grain growth, thus degrading the superconducting properties; hence, the critical current densities are reduced.

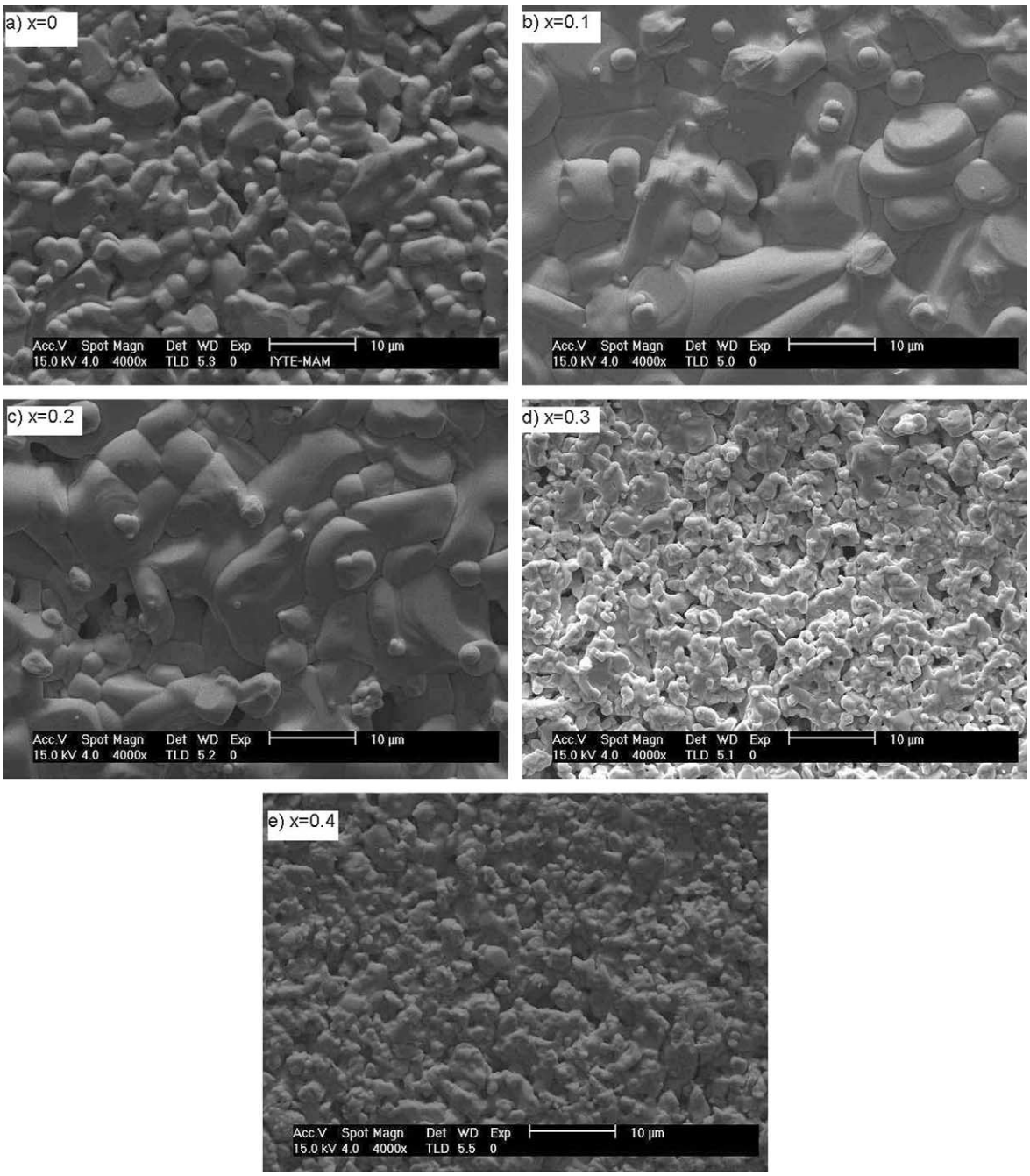

Fig. 4. SEM micrographs of pure and Ag doped YBCO samples with different Ag concentration: (a) $x = 0$, (b) $x = 0.1$, (c) $x = 0.2$, (d) $x = 0.3$ and (e) $x = 0.4$.

As shown in Fig. 5(c), the normalized critical current density, $J_c(B)/J_c(0)$, were plotted against magnetic field, B at 77 K. In which, the magnetic field dependencies of the critical current densities of the samples doped with different amount of Ag are clearly exhibited. As we expect, the sample C showed the slowest J_c drop under applied field. Here, we conclude that the magnetic field dependence of J_c in YBCO compounds decreases with the Ag doping increases up to an optimum amount. In bulk YBCO composites, magnetic flux penetration also occurs through the micro-cracks. In addition to the improvement on the grain structure, Ag addition also

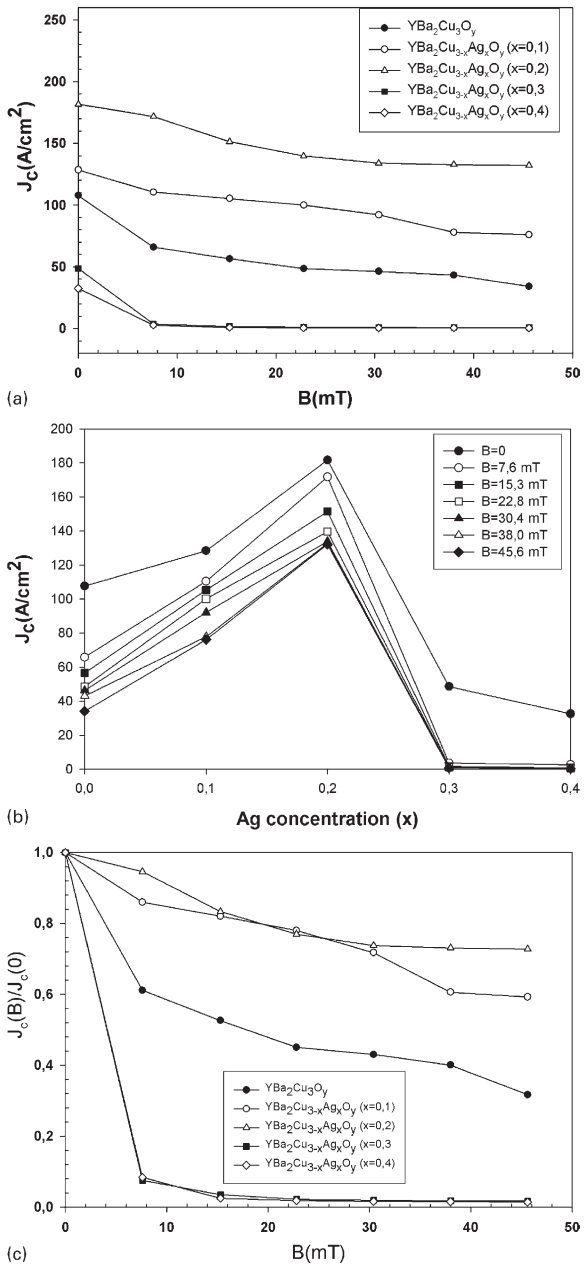

Fig. 5. (a) Critical current density, J_c, versus magnetic field, B, dependence of pure and Ag doped YBCO samples at 77 K, (b) critical current density, J_c, versus Ag doping concentration, x, dependence of samples at 77 K, (c) the normalized critical current density, $J_c(B)/J_c(0)$, versus magnetic field, B at 77 K.

reduces the micro-crack formation hence modifying the structure. This means that Ag precipitates reduce the effect of inter-grain weak-links and enhance the effectiveness of pinning centers.

4. Conclusion

In this study, we investigated the effect of Ag doping on the superconducting and transport properties of YBCO ceramics. The improvement in the microstructure and in the superconducting properties of the samples was observed with the variation of cationic ratio of Ag up to $x = 0.2$. The critical current density of the sample C enhanced by the factor of 169% at 77 K and $B = 0$ mT. By the investigation of magnetic field dependence of the critical current density, we observed that the J_c versus B dependency decreases with increasing of Ag content up to $x = 0.2$. This indicates that the Ag doping improves the grain growth and their orientations, and modifies the inter-grain weak-links. In the temperature processing of YBCO ceramics, liquid Ag fills into the pores of the structure and modifies the micro-cracks, thus strengthening the role of pinning centers. However, when the Ag content exceeds $x = 0.2$, the structure and thus the superconducting properties of the samples deteriorate. The excess amount of silver plays a role of preventing factor for the growth of YBCO grains. Consequently, grains become smaller and arbitrarily oriented hence showing lower performance for the high current applications.

Acknowledgements

The authors would like to express their gratitude to specialists at the Material Research Center at Izmir Institute of Technology for their valuable suggestions in the analysis of SEM and XRD.

References

[1] C. Leblond-Harris, R. Caillard, I. Monot-Laffez, G. Desgardin, B. Raveau, Physica C 341–348 (2000) 2439–2440.
[2] Y. Li, J.R. Liu, X.T. Cui, Y. Cao, Z.J. Qu, Q.Y. Chen, C.W. Chu, W.K. Chu, Physica C 282–287 (1997) 653–654.
[3] C. Harnois, G. Desgardin, I. Laffez, X. Chaud, D. Bourgault, Physica C 383 (2002) 269–278.
[4] T. Puig, P. Rodriguez Jr., A.E. Carrillo, X. Obradors, H. Zheng, U. Welp, L. Chen, H. Claus, B.W. Veal, G.W. Crabtree, Physica C 363 (2001) 75–79.
[5] E. Mendoza, T. Puig, E. Varesi, A.E. Carrillo, J. Plain, X. Obradors, Physica C 334 (2000) 7–14.
[6] M.M. Abdelhadi, Kh.A. Ziq, Supercond. Sci. Technol. 7 (1994) 99–102.
[7] Y. Matsumoto, M. Koinuma, H. Yamamoto, T. Nishimori, Solid State Ionics 95 (1997) 309–314.
[8] P.L. Villa, G. Taglieri, F. D'Orazio, F. Lucari, G. Santella, L. Catoni, S. Lozzi, J. Magn. Magn. Mater. 226-230 (2001) 314–315.